

Supplementary Information

Triggering the Dynamics of a Carbazole-p- [phenylene-diethynyl]-xylene Rotor through a Mechanically Induced Phase Transition

*Andrés Aguilar-Granda,^a Abraham Colin-Molina,^a Marcus J. Jellen,^b Alejandra Núñez-Pineda,^{a,c} Miguel Eduardo Cifuentes-Quintal,^d Rubén Alfredo Toscano,^a Gabriel Merino,^d
Braulio Rodríguez-Molina^{*a}*

^aInstituto de Química, Universidad Nacional Autónoma de México, Circuito Exterior, Ciudad Universitaria, 04510, Ciudad de México, México. ^bDepartment of Chemistry and Biochemistry, University of California, Los Angeles, California 90095, United States. ^cCentro Conjunto de Investigación en Química Sustentable UAEM-UNAM, Carretera Toluca-Atlacomulco km 14.5, Toluca, 50200, Estado de México, México. ^dDepartamento de Física Aplicada, Centro de Investigación y de Estudios Avanzados, Unidad Mérida. Km 6 Antigua Carretera a Progreso. Apdo. Postal 73, Cordemex, 97310, Mérida, Yuc., México.

^{*}brodriguez@iquimica.unam.mx

Contents

Single crystal X-Ray Diffraction	S2
Thermal analyses	S6
Powder X-ray Diffraction	S9
Solution ^{13}C assignment and chemical shift of compound 2.....	S12
Solid state ^{13}C Nuclear Magnetic Resonance	S13
Solid state ^2H NMR Nuclear Magnetic Resonance	S14
Computational section.....	S18
Experimental section	S20

Single crystal X-Ray Diffraction

Data collection were performed at 298 K and 150 K on a Bruker-D8-Venture diffractometers with Cu $\text{K}\alpha$ -radiation, $\lambda = 1.54178 \text{ \AA}$ and a Bruker Smart APEX II CCD diffractometer with graphite-monochromatic Mo $\text{K}\alpha$ -radiation, $\lambda = 0.71073 \text{ \AA}$. The structures were solved by direct methods and refined using SHELXL-2014. All non-hydrogen atoms were refined anisotropically.

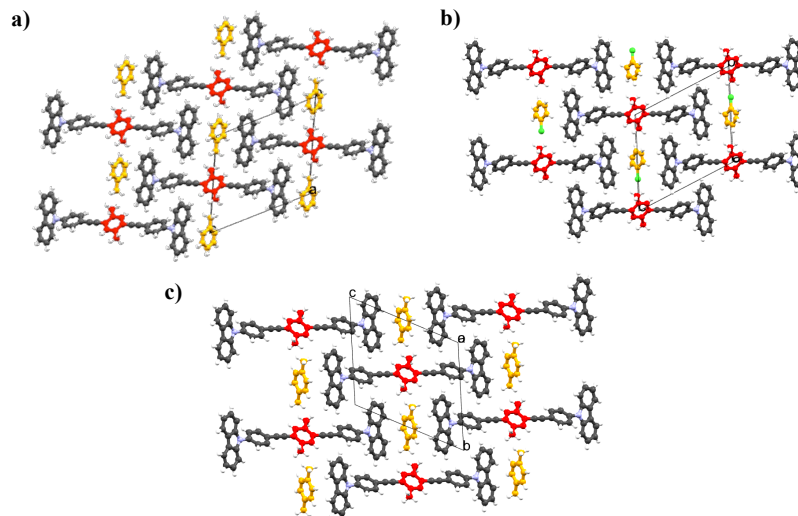


Figure S1. Crystal packing of compound **2** obtained from aromatic solvents (Group A): a) toluene (Form I), b) chlorobenzene (Form II), c) *p*-Xylene (Form III).

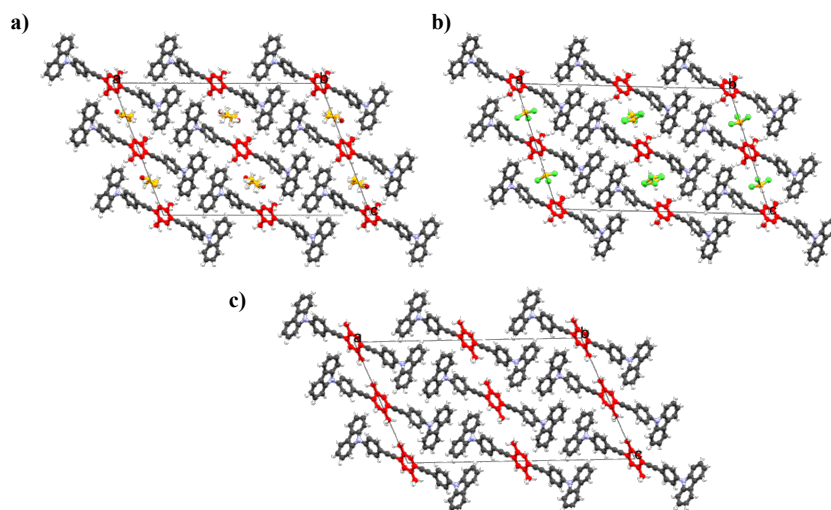


Figure S2. Crystal packing of rotor **2** obtained of aliphatic solvents (Group B): a) THF (Form IV), b) chloroform (Form V) and c) solvent free (Form VI).

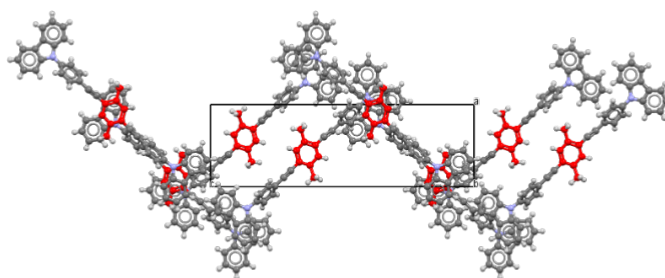


Figure S3. Crystal packing of solvent-free form VII obtained from heating Form VI.

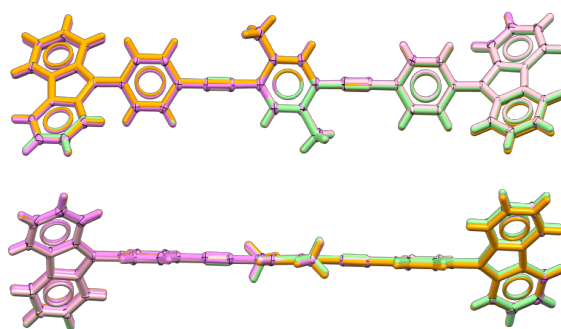


Figure S4. *Molecular overlay of compound 2 form VI at different temperatures (295, 230, 165 and 100 K)*

Table S1. *Crystallographic data for the solid forms obtained of compound 2.*

Compound	Form I Toluene	Form II Cl-benzene	Form III <i>p</i> -xylene	Form IV THF	Form V Chloroform	Form VI Solvent free	Form VII Solvent free	Form VIII Solvent free
Formula	C ₅₅ H ₄₀ N ₂	C ₅₄ H ₃₇ ClN ₂	C ₅₆ H ₄₂ N ₂	C ₅₂ H ₄₀ N ₂ O	C ₄₉ H ₃₃ Cl ₃ N ₂	C ₄₈ H ₃₂ N ₂	C ₄₈ H ₃₂ N ₂	C ₄₈ H ₃₂ N ₂
MW/g mol ⁻¹	728.89	749.31	742.92	708.86	756.12	636.75	636.75	636.75
Crystal system	Triclinic	Triclinic	Triclinic	Monoclinic	Monoclinic	Monoclinic	Orthorhombic	Monoclinic
Space group	<i>P</i> -1	<i>P</i> -1	<i>P</i> -1	<i>C</i> 2/ <i>c</i>	<i>C</i> 2/ <i>c</i>	<i>C</i> 2/ <i>c</i>	<i>P</i> 2 ₁ 2 ₁ 2 ₁	
<i>a</i> /Å	5.4663(9)	5.4423 (1)	5.5357 (5)	32.439 (7)	33.601(2)	34.450(10)	9.6185(5)	5.403
<i>b</i> /Å	14.046(2)	14.0101 (3)	13.9222 (14)	5.7640 (1)	5.769(3)	5.403(3)	11.6931(7)	17.414
<i>c</i> /Å	15.063(3)	15.0265 (3)	15.0956 (15)	22.026 (5)	20.723	19.982(5)	30.72126(1)	19.975
α (°)	114.834(4)	114.802 (1)	115.448 (2)	90	90	90	90	90
β (°)	90.234(5)	90.263 (2)	90.571 (2)	111.05 (5)	109.430 (5)	113.075(19)	90	112.716
γ (°)	101.595(5)	101.034 (2)	97.252 (2)	90	90	90	90	90
<i>V</i> /Å ³	1023.05	1016.01	1039.44	3843.5	3788.6	3421.75	3455.3	1709.10
<i>Z</i>	1	1	1	4	4	4	4	-
<i>Z'</i>	0.5	0.5	0.5	0.5	0.5	0.5	1	-
ρ /g cm ⁻³	1.333	1.369	1.187	1.350	1.411	1.236	1.224	-
Collected Refl.	3764	3835	5594	3594	3440	3893	7981	-
Ind. Ref. (<i>R</i> _{int})	2508	0.1143	2748	2746	1438	3012	2728	-
$R[F^2 > 2\sigma(F^2)]$	0.0574	0.0626	0.0551	0.0515	0.0839	0.0448	0.0849	-
<i>R</i> _w (all data)	0.1493	0.0875	0.1280	0.0682	0.2328	0.0591	0.2871	-
$\Delta\rho_{\text{max}}/e \text{ Å}^{-3}$	0.997	0.949	0.999	0.985	0.985	0	0.996	-
$\Delta\rho_{\text{min}}/e \text{ Å}^{-3}$	0.986	0.792	0.084	0.981	0.953	0	0.993	-
<i>T</i> (K)	298	298	298	150	150	150	298	-

Thermal analyses

Differential scanning calorimetry and thermogravimetric analyses of a crystalline sample of **2** was carried out on a Netzsch STA 449 F3 Jupiter thermal analyzer under nitrogen atmosphere, with a heating rate of 10 °C/min.

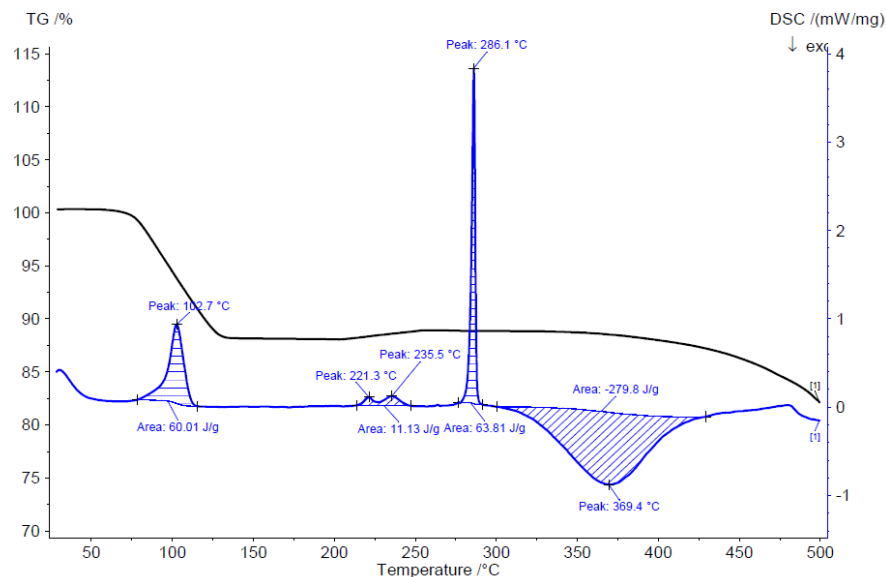


Figure S5. TGA (black line) and DSC (blue line) of the toluene solvate (Form I).

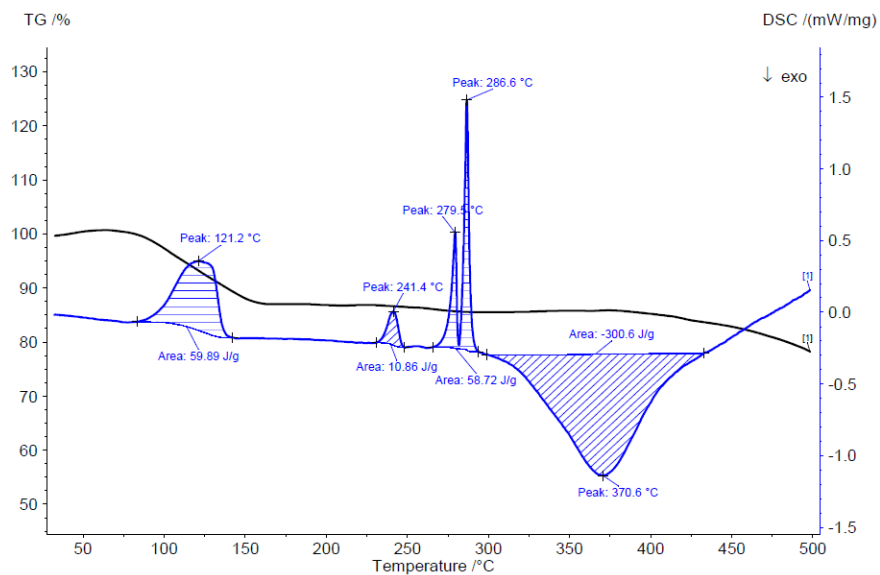


Figure S6. TGA (black line) and DSC (blue line) of the chlorobenzene solvate (Form II).

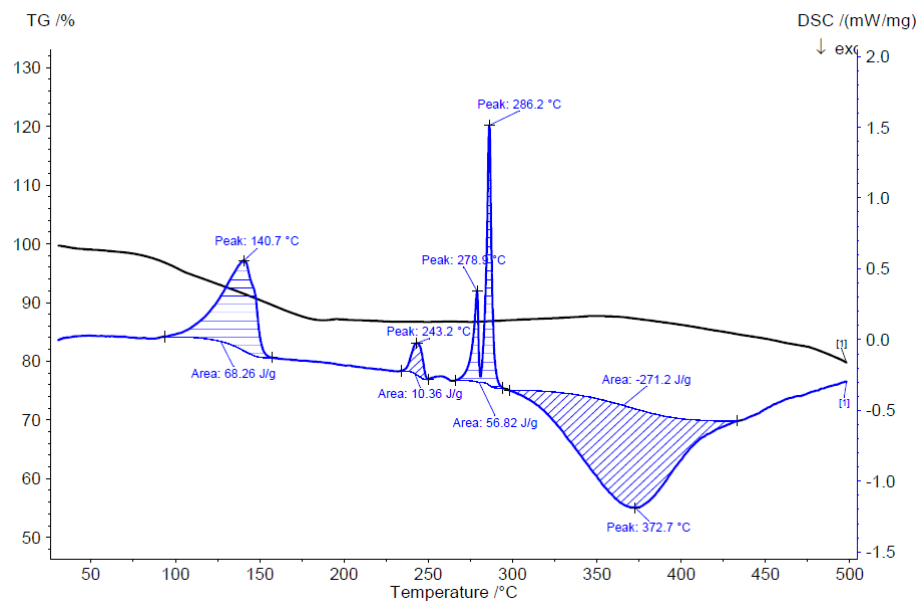


Figure S7. TGA (black line) and DSC (blue line) of the p-Xylene solvate (Form III).

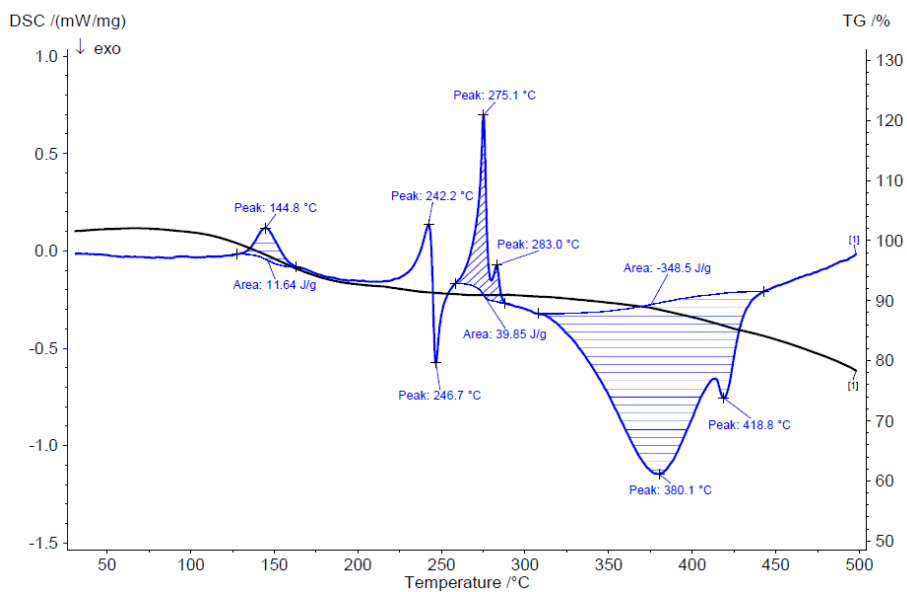


Figure S8. TGA (black line) and DSC (blue line) of the THF solvate (Form IV).

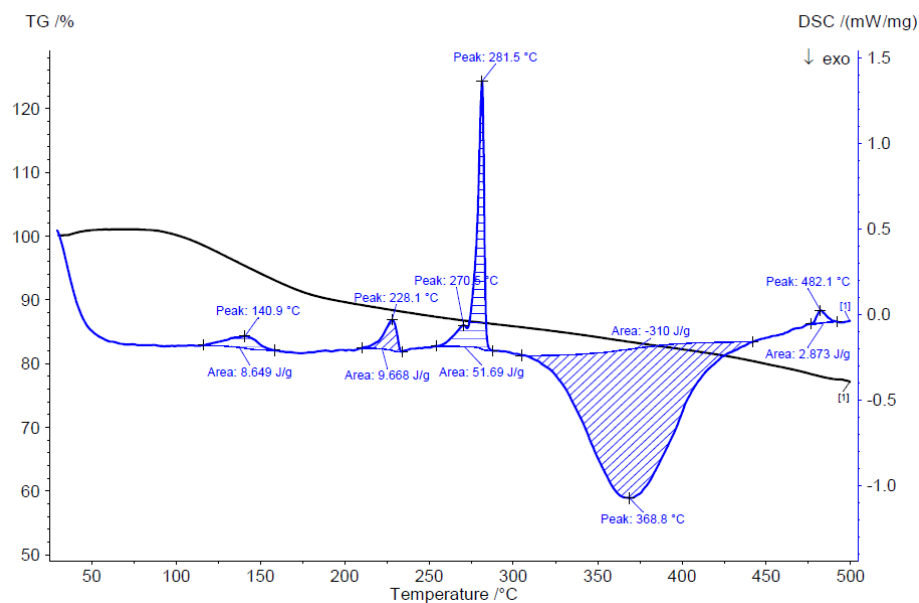


Figure S9. TGA (black line) and DSC (blue line) of the chloroform solvate (Form V).

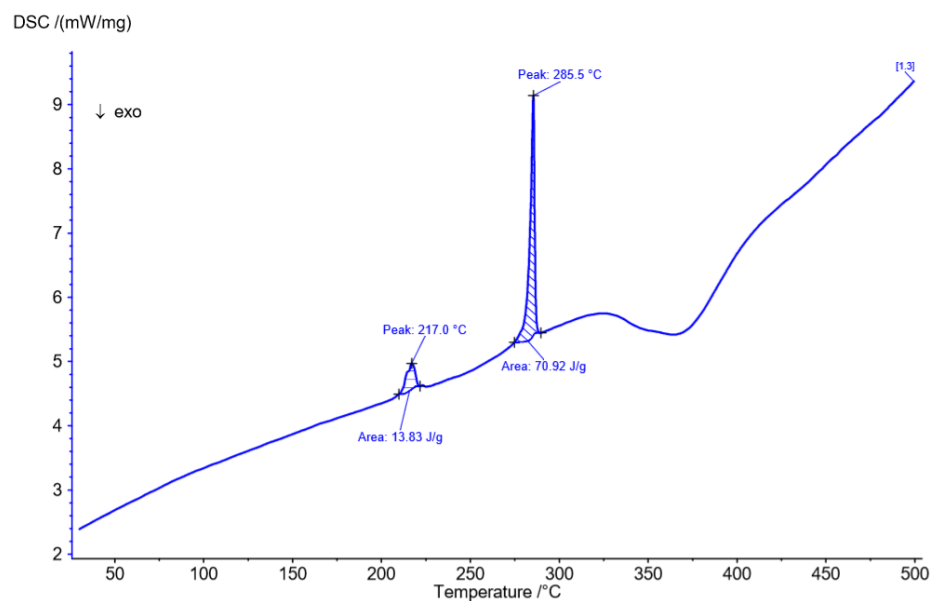


Figure S10. DSC of the solvent free structure (Form VI).

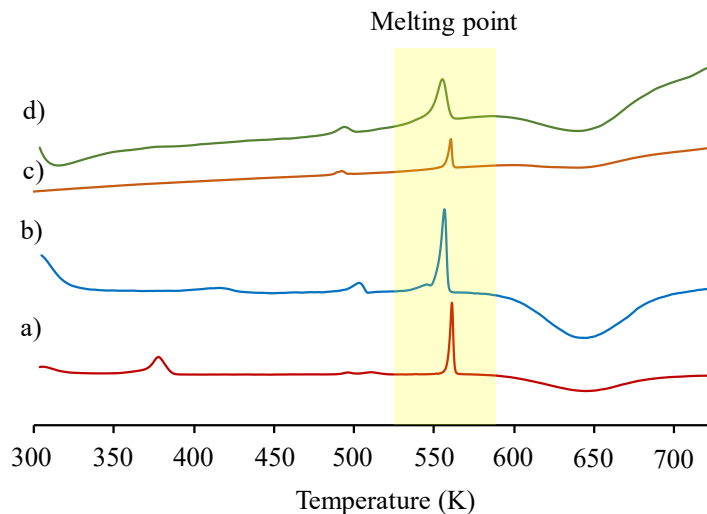


Figure S11. Comparison of DSC analyses of forms a) I, b) V, c) VII and d) VIII.

Powder X-ray Diffraction

Analyses were carried out using $\text{Cu-K}\alpha_1 = 1.5406 \text{ \AA}$ radiation, data were collected at room temperature in the range of $2\theta = 5\text{--}35^\circ$ (step of 0.017° , step time 40.005 s). Calculations of crystallinity percentage in the several batches (A, B and C) were carried out using the fullprof program selecting background points corresponding to the amorphous phase part of the compound and calculating the crystallinity as follows: *integration of the amorphous phase intensities (a); integration of the sample intensities (s)*. Crystallinity rate = $1 - a/s$.

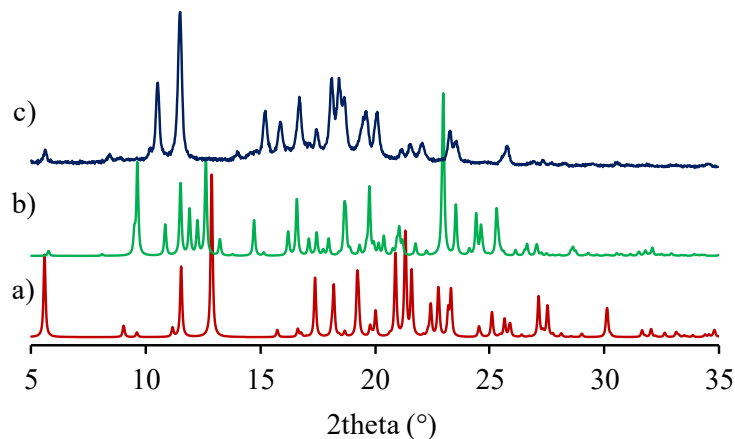


Figure S12. Comparison of Powder X-ray diffraction patterns of solvent free structures: a) Form VI (calculated), b) Form VII (calculated) and c) Form VIII (experimental).

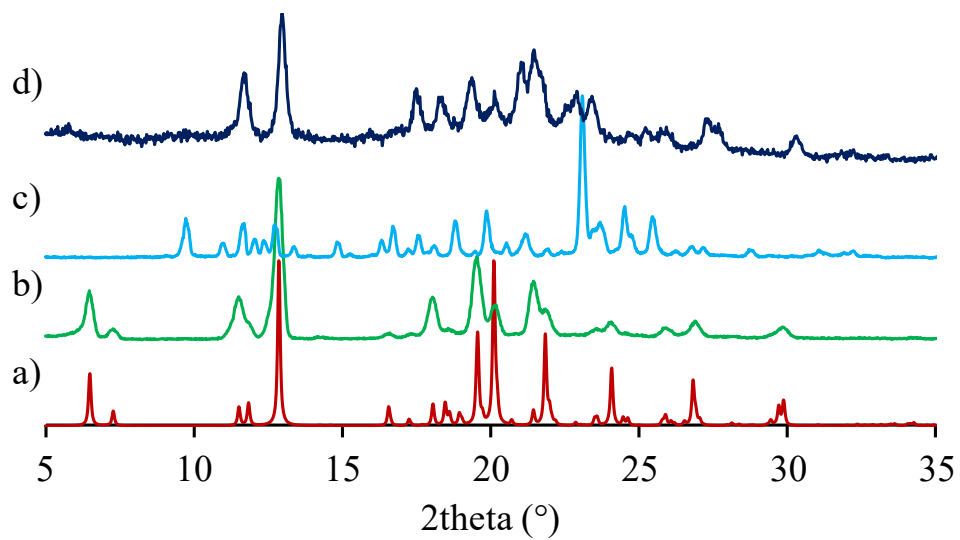


Figure S13. Comparison of Powder X-ray diffraction patterns. Calculated: a) Form I
Experimental: b) Form I c) Form VII and d) Form VIII.

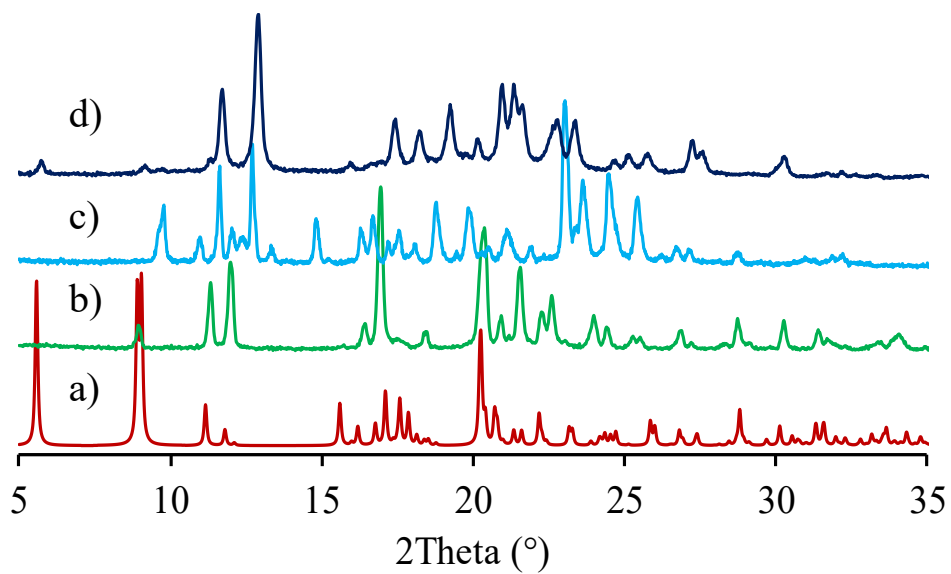


Figure S14. Comparison of Powder X-ray diffraction patterns. Calculated: a) Form V
Experimental: b) Form V c) Form VII and d) Form VIII.

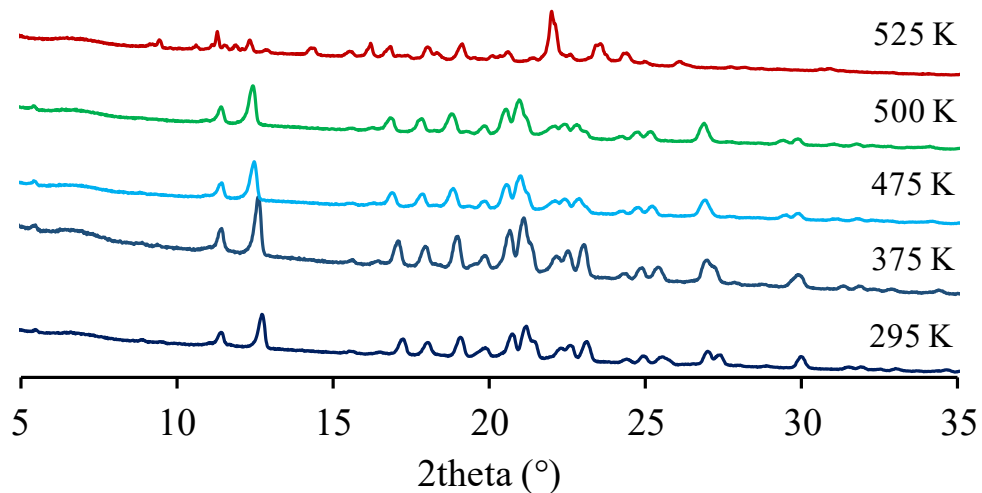


Figure S15. Powder X-ray diffraction at variable temperature from Form VI (295 K) to Form VII (525 K)

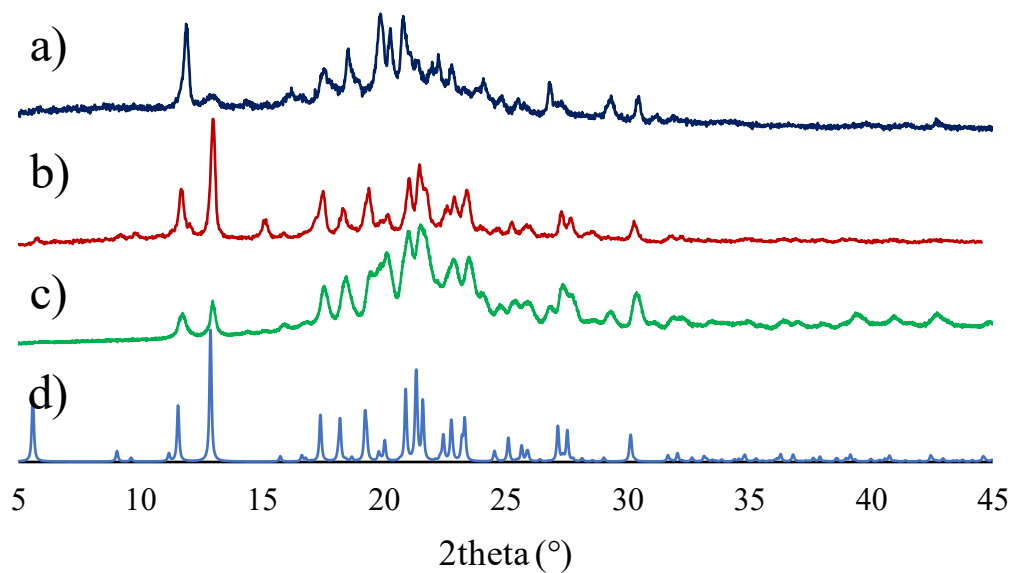


Figure S16. Comparison of Powder X-ray Diffraction patterns for compound **2** solvent free form **VIII** of several batches **A** (a), **B** (b) and **C** (c) and pattern calculated from crystal structure optimized (d) from DFT computations.

Solution ^{13}C assignment and chemical shift of compound **2**

Table S2. NMR data for the unequivocal ^{13}C assignment of compound **2** using the HMBC experiment.

Position	δ (ppm)	Multiplicity	^1H (ppm) [J - Hz]	HMBC (ppm) [correlation]
1	109.7	CH	H-1, m (7.47-7.39)	H-3 (7.33-7.28) [3]
2	126.1	CH	H-2, m (7.47-7.39)	H-4 (8.15) [3]
3	120.2	CH	H-3, m (7.33-7.28)	H-1 (7.47-7.39) [3]
4	120.4	CH	H-4, d (8.15), [7.7]	H-2 (7.47-7.39) [3]
4a	123.6	C		H-1 (7.47-7.39) [3], H-3 (7.33-7.28) [3]
9a	140.6	C		H-1 (7.47-7.39) [2], H-2 (7.47-7.39) [3], H-4 (8.15) [3]
10	137.5	C		H-11 (7.69) [2], H-12 (7.69) [3]
11	126.9	CH	H-11, AA'XX' (7.69), [8.6]	
12	133.0	CH	H-12, AA'XX' (7.69), [8.6]	
13	122.3	C		H-11 (7.69) [3]
14	94.0	C		H-12 (7.69) [3]
15	89.2	C		H-19 (7.47-7.39) [3]
16	123.0	C		H-18 (2.55) [3], H-19 (7.47-7.39) [2]
17	137.6	C		H-18 (2.55) [2], H-19 (7.47-7.39) [3]
18	20.1	CH ₃	H-18, s (2.55)	

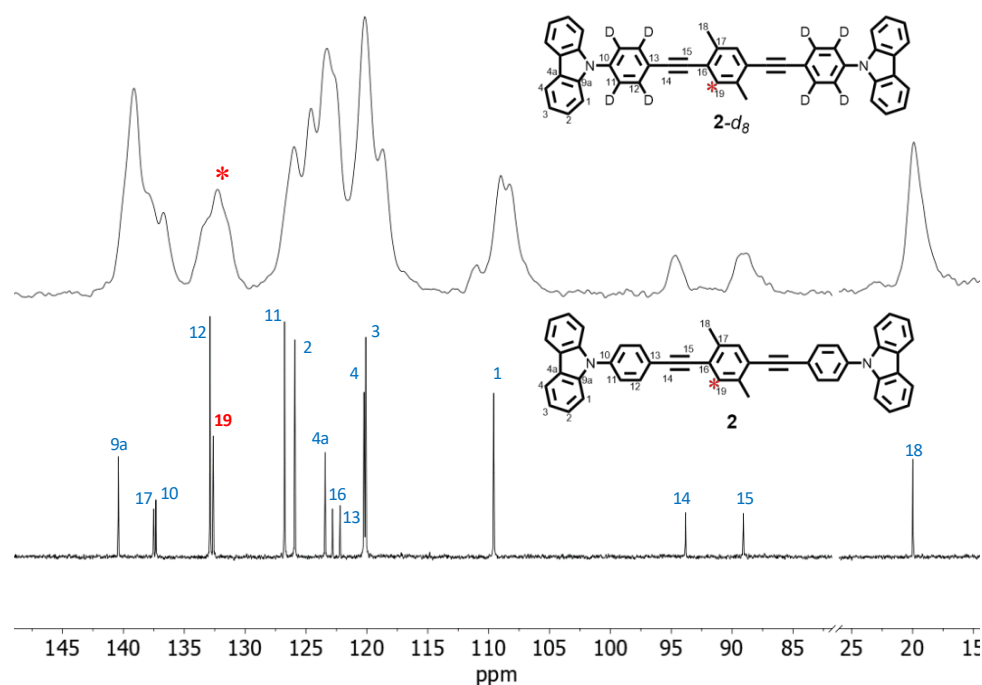


Figure S17. Assignment of the ^{13}C peaks of compound **2** in solution and in the solid state (by comparison).

Solid state ^{13}C Nuclear Magnetic Resonance

The spectra were recorded with natural abundance ^{13}C powdered samples spun at 10 kHz on an AV600 solid-state spectrometer utilizing 3.2 mm HXY CP/MAS probe at 150.93 MHz. A contact time of 2 ms and a delay of 2.5 s between pulses were used to acquire the spectra. The ^{13}C NMR chemical shifts were referenced using the resonances of solid adamantane at 37.7 and 28.7 ppm. Temperature readings were calibrated with ^{207}Pb CPMAS NMR of $\text{Pb}(\text{NO}_3)_2$ at various temperatures.

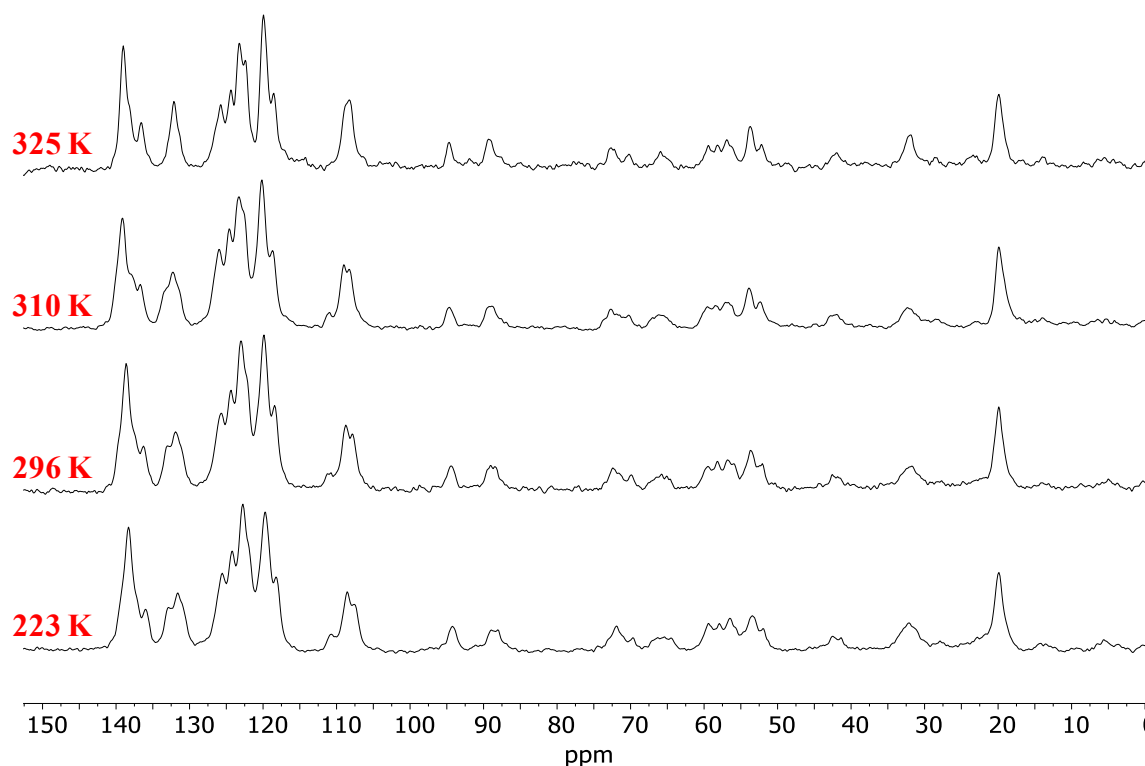


Figure S18. VT ^{13}C CPMAs experiments of compound **2-d₈**.

Solid state ^2H NMR Nuclear Magnetic Resonance

The solid-state ^2H NMR (SS ^2H NMR) spin-echo experiments in this work were performed on a Bruker AV600 instrument at 92.1 MHz (deuterium resonance frequency) with a 5 mm wide-line probe and 90-degree pulse of 2.9 μs . To suppress the undesired artifacts, a quadrupolar-echo sequence with phase recycling was used. An echo delay of 50 μs was used after the refocusing delay of 46 μs , and the recycle delay between pulses was 15 s. In the experiment, about 50 mg of batch B and 20 mg of batch C were placed in separate, short borosilicate glass NMR tube. 256 and 512 scans were acquired for batch B and C, respectively, for all temperatures explored. All spectra in this work were obtained using a line broadening of 3.0 kHz in data processing. The calculated ^2H NMR line shapes for the different batches of the rotor (A, B, C) were simulated using the NMRweblab 6.6,¹ applying a QCC of 176 kHz with distorted cone angle of 54.7° and angular displacements of 90° (4-fold), based on a symmetrical potential with populations 0.25:0.25:0.25:0.25 and pulse delay of 50 μs . The simulations of every batch were carried out considering a rigid contribution in % that corresponded to the same percentage of crystalline

¹ <http://weblab.mpip-mainz.mpg.de/weblab66/>

component as determined by powder X-ray diffraction experiments. The variables were the different rotation frequencies showing the growth of the narrow signal.

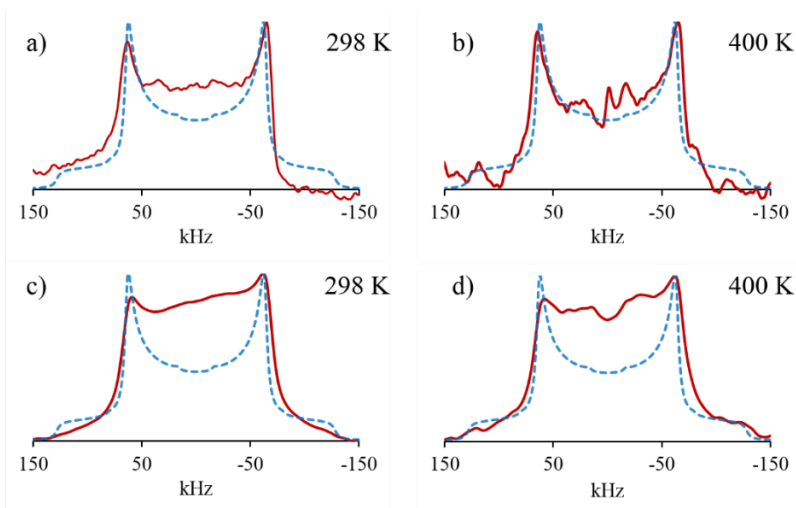


Figure S19. Line shape analysis of ^2H NMR spectra: a) Toluene solvate (Form I) b) Form VII verified by PXRD (desolvated from the toluene solvate) c) Solvent-free Form VI at room temperature and d) Form VI at high temperature without phase transition.

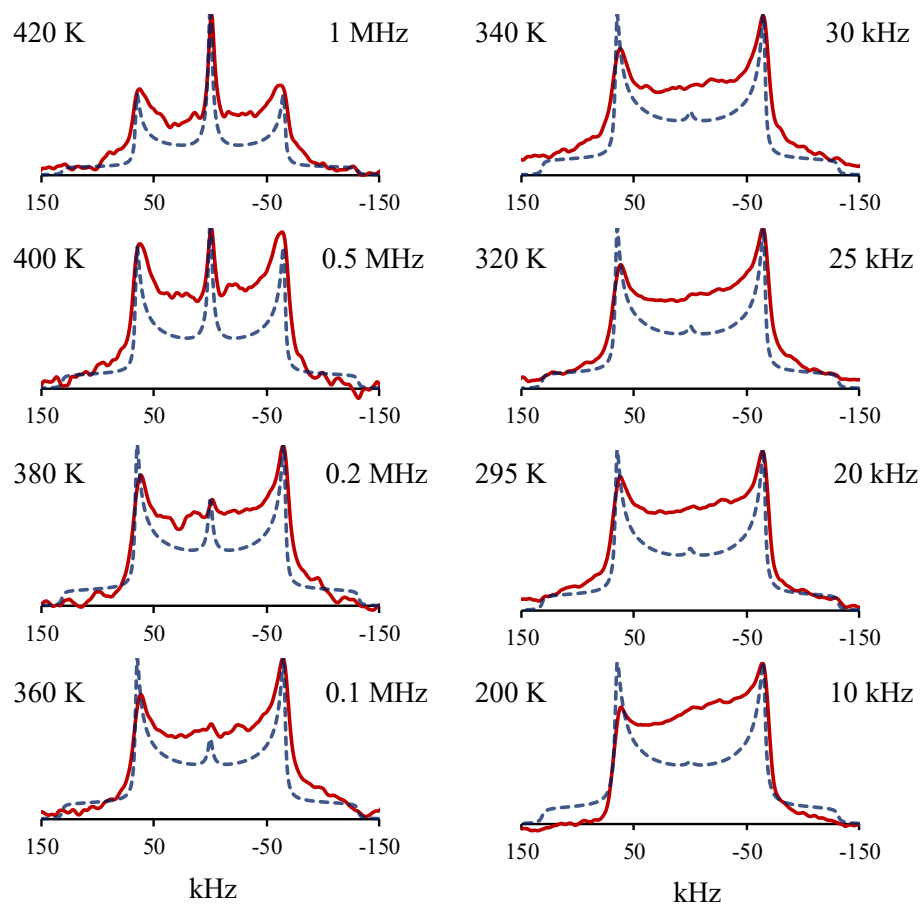


Figure S20. Line shape analyses of the VT ^2H NMR spectra of compound **2** with a mixture of form VIII/amorphous solid (batch B).

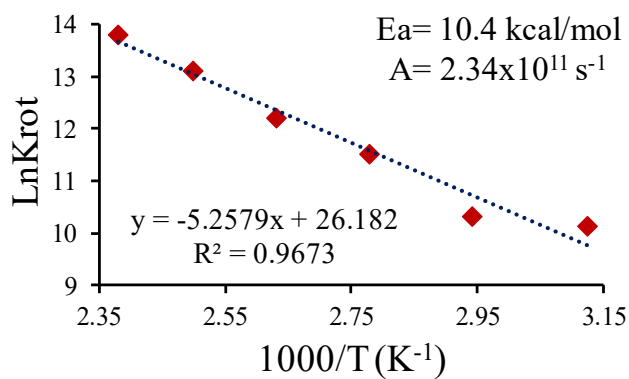


Figure S21. Arrhenius plot of the motion in **2** with a mixture of form VIII/amorphous solid (batch B)

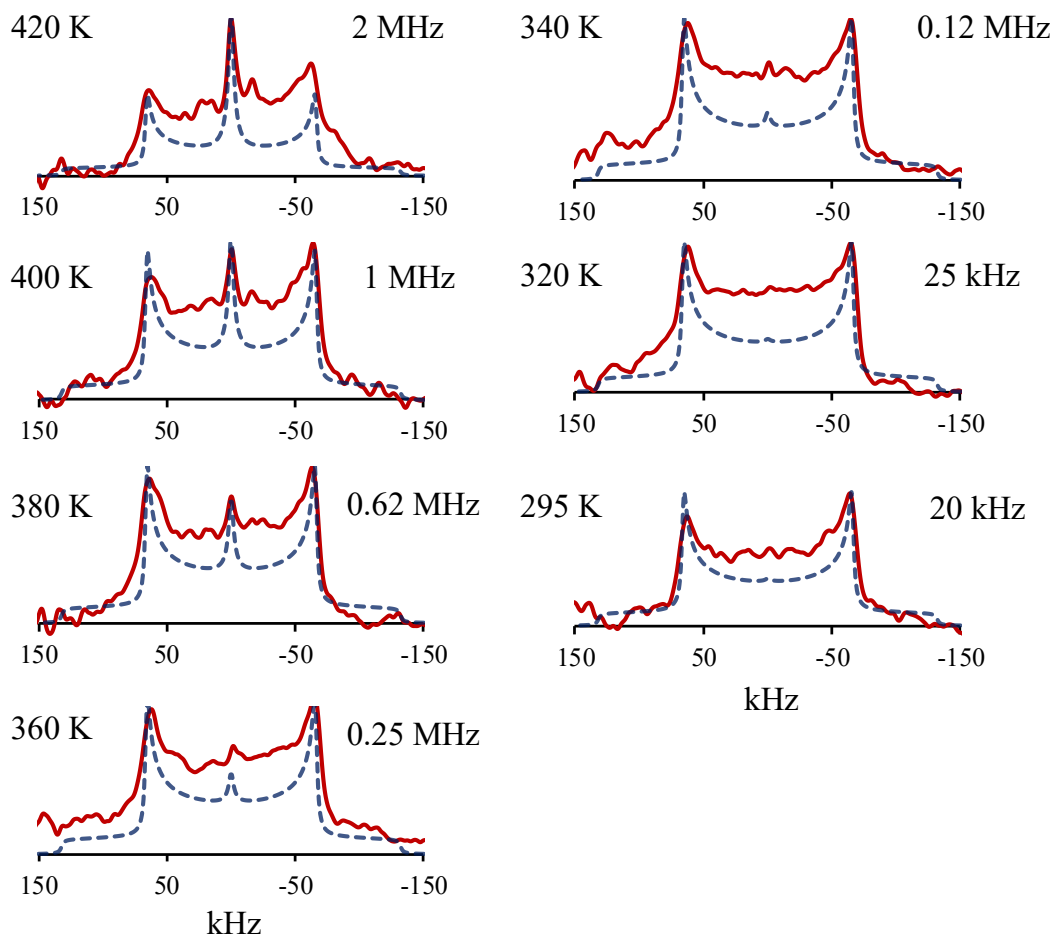


Figure S22. Line shape analysis of ^2H NMR spectra at variable temperature of compound **2** with a mixture of form VIII/amorphous solid (batch C)

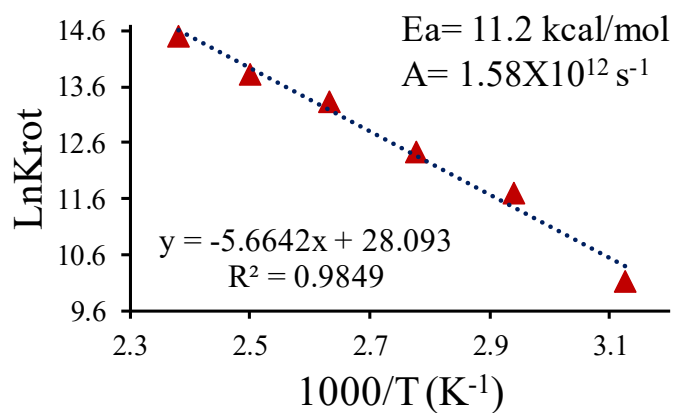


Figure S23. Arrhenius plot of the motion in **2** a mixture of form VIII/amorphous solid (batch C)

Table S3. Activation parameters for every batch of molecular rotor **2** a mixture of form VIII/amorphous solid

Batch	Crystalline (%)	Amorphous (%)	Activation Energy (kcal/mol)	Pre-exponential Factor (s ⁻¹)
A	17	83	7.4	6.22x10 ¹⁰
B	24	76	10.4	2.34x10 ¹¹
C	42	58	11.2	1.58x10 ¹²

Computational section

Frontier orbitals were obtained using DFT calculations performed with Gaussian 16 (version A.03) package.² All structures were optimized used a 6-311++G(d,p) basis set. The global hybrid functional B3LYP was used for HOMO-LUMO calculations.

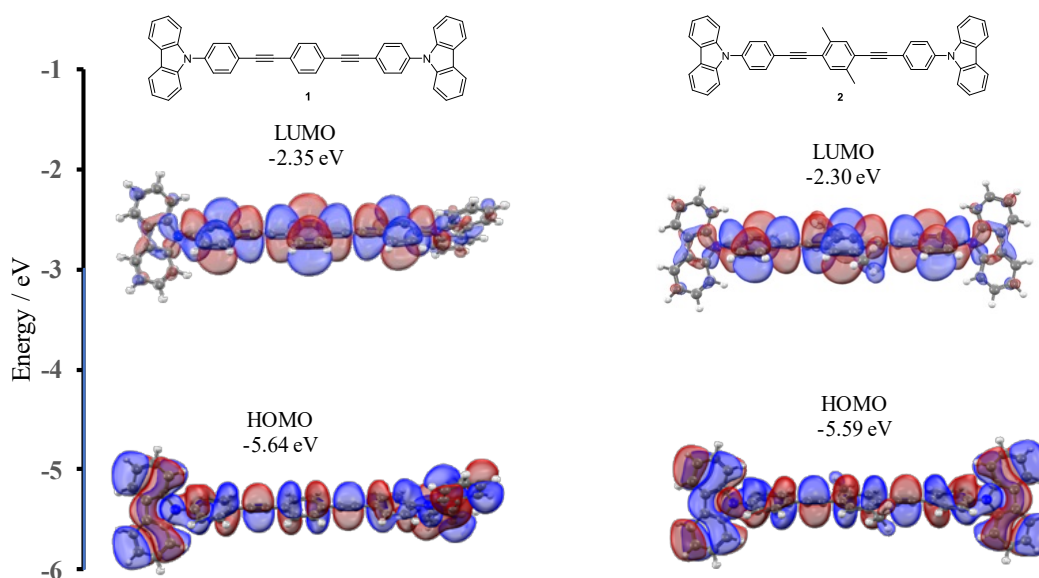


Figure S24. Electron distribution both HOMO/LUMO state of molecules **1** and **2** in gas phase.

² M. J. Frisch, G. W. Trucks, H. B. Schlegel, G. E. Scuseria, M. A. Robb, J. R. Cheeseman, G. Scalmani, V. Barone, G. A. Petersson, H. Nakatsuji, X. Li, M. Caricato, A. V. Marenich, J. Bloino, B. G. Janesko, R. Gomperts, B. Mennucci, H. P. Hratchian, J. V. Ortiz, A. F. Izmaylov, J. L. Sonnenberg, D. Williams-Young, F. Ding, F. Lipparini, F. Egidi, J. Goings, B. Peng, A. Petrone, T. Henderson, D. Ranasinghe, V. G. Zakrzewski, J. Gao, N. Rega, G. Zheng, W. Liang, M. Hada, M. Ehara, K. Toyota, R. Fukuda, J. Hasegawa, M. Ishida, T. Nakajima, Y. Honda, O. Kitao, H. Nakai, T. Vreven, K. Throssell, J. A. Montgomery, Jr., J. E. Peralta, F. Ogliaro, M. J. Bearpark, J. J. Heyd, E. N. Brothers, K. N. Kudin, V. N. Staroverov, T. A. Keith, R. Kobayashi, J. Normand, K. Raghavachari, A. P. Rendell, J. C. Burant, S. S. Iyengar, J. Tomasi, M. Cossi, J. M. Millam, M. Klene, C. Adamo, R. Cammi, J. W. Ochterski, R. L. Martin, K. Morokuma, O. Farkas, J. B. Foresman, and D. J. Fox, Gaussian, Inc., Wallingford CT, 2016.

The rotational potential for the solvent free forms was computed using density functional theory calculations within the framework of the Projector-Augmented Wave (PAW) method,³ as implemented in the Vienna Ab-initio Simulation Package (VASP).⁴ The electron-ion interactions were described using the PAW potentials from the VASP library.⁵ Valence states were expanded in plane waves with an energy cut-off of 550 eV. In all the calculations we used the GGA-PBE exchange-correlation functional,⁶ augmented by the Grimme's D3-dispersion correction.^{7,8} The integration in the Brillouin zone was performed using a $3\times 1\times 1$ Monkhorst-Pack k-point mesh for the forms VI and VIII, and $2\times 2\times 1$ for the form VII. The structural parameters were computed by a variable-cell optimization until all forces were smaller than 0.002 eV/Å (see Table S2). As starting geometries, we used the experimental information at room temperature. In the case of form VIII, we fixed the lattice parameter and optimized the atomic positions until our calculations match the experimental powder X-ray diffraction patterns.

The rotational potentials were computed by simultaneously rotating the two phenylenes attached to the carbazole stators. During this process we allow the relaxation of all the other atoms and molecules. We considered two angular trajectories: both the phenylenes simultaneously rotate in the same direction (conrotatory) or the opposite direction (disrotatory). The rotational potentials with the minimum energy barriers are presented in Figure S25, and correspond to disrotatory movement for forms VI and VIII, and conrotatory for form VII. The molecular distortions during rotation in form VIII are shown in Movies S1-S3. For a better appreciation of the molecular axis distortion during rotation, in Movies S1 and S2 we show only two adjacent molecular rotors. The cooperative displacement among all the molecular rotors in the crystal unit cell is presented in Movie S3.

³ P.E. Blöchl, Phys. Rev. B, 1994, **50**, 17953

⁴ G. Kresse, J. Furthmüller, Phys. Rev. B, 1996, **54**, 11169.

⁵ G. Kresse, and J. Joubert, Phys. Rev. B, 1999, **59**, 1758.

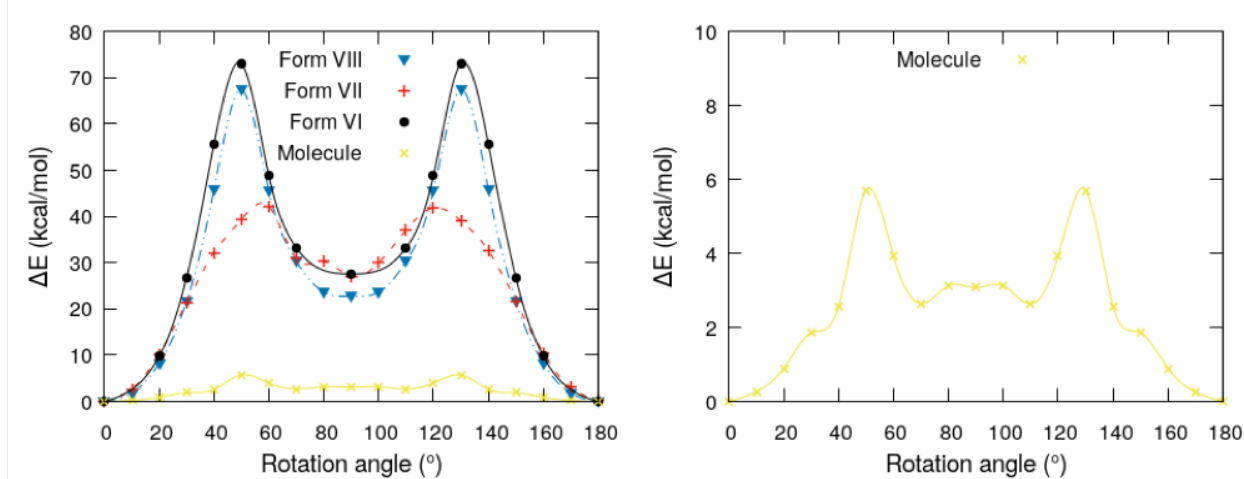
⁶ J. P. Perdew, K. Burke, and M. Ernzerhof, Phys. Rev. Lett., 1996, **77**, 3865.

⁷ S. Grimme, J. Antony, S. Ehrlich, and S. Krieg, J. Chem. Phys., 2010, **132**, 154104.

⁸ S. Grimme, S. Ehrlich, and L. Goerigk, J. Comp. Chem. **32**, 2011, 1456.

Table S4. Computed lattice parameters for form VI, VII and VIII

Form	a (Å)	b (Å)	c (Å)	α (°)	β (°)	γ (°)	Volume (Å ³)
VI	34.4510	5.3271	19.9397	90.000	114.001	90.000	3343.02
VII	9.4867	11.5963	29.9623	90.000	90.000	90.000	3296.1527
VIII	5.4036	17.4141	19.9747	90	112.716	90	1709.10

**Figure S25.** Left: Rotational potentials for forms **VI**, **VII**, and **VIII**. Right: Rotational potential of the rotor **2** in the gas phase.

Experimental section

All reagents were purchased from Sigma-Aldrich and used as received. Reactions were monitored by TLC on silica gel plates 60 F₂₅₄ and the spots were detected by UV. Inert atmosphere reactions were carried out under nitrogen. ¹H and ¹³C NMR spectra were recorded at ambient temperature using Bruker Fourier 300 and Bruker Fourier 400 spectrometers referenced to TMS (0.0 ppm) and CDCl₃ (77.0 ppm) respectively, unless otherwise noted. Uncorrected melting points were determined in a Fisher Johns melting point apparatus. HRMs were obtained by Direct Analysis in Real Time (DART) in a Jeol JMS-AccuTOF.

1,4-bis(carbazol-9-yl)phenyl)ethynyl)-2,5-dimethylbenzene (2)

Under nitrogen atmosphere in a two-neck round-bottom flask, a mixture of N-(4-iodophenyl)carbazole) (**3**) (0.500 g, 1.35 mmol), 1,4-diethynyl-2,5-dimethylbenzene (**4**) (0.104 g,

0.677 mmol), PdCl₂(PPh₃)₂ (0.095 g, 0.135 mmol), CuI (0.012 g, 0.067 mmol), dry THF (6 mL) and triethylamine (1 mL) was stirred for 3 h at room temperature, then the mixture was washed with 30 mL of saturated solution of NH₄Cl and the organic phase was extracted with dichloromethane (3x30 mL). The organic phase was dried over Na₂SO₄ and the solvent was removed by evaporation. The crude product was purified by column chromatography using a mixture hexanes/dichloromethane (95:5) as eluent to afford compound **2** as a yellow solid (0.341 g, 64 %, M.P. by DCS 278-285 °C). IR ν_{max} : 3048.7, 3022.6, 2919.6, 2203.4, 2057.4, 2035.3, 2013.3, 1966.2, 1712.4, 1595.6, 1513.0, 1447.2, 1223.6, 1014.7, 832.8, 747.5, 723.0, 620.5. ¹H NMR (300 MHz, CDCl₃) δ : 8.15 (d, 2H, ³J = 7.7 Hz), 7.77 (d, 2H, ³J = 8.6 Hz), 7.59 (d, 2H, ³J = 8.6 Hz), 7.44 (m, 5H), 7.31 (m, 2H), 2.54 (s, 3H). ¹³C NMR (75 MHz, CDCl₃) δ : 140.6 (C9a), 137.6 (C10), 137.5 (C17) 133.0 (C12), 132.8 (C19), 126.9 (C11), 126.1 (C2), 123.6 (C4a), 123.0 (C16), 122.3 (C13), 120.4 (C4), 120.2 (C3), 109.7 (C1), 94.0 (C14), 89.2 (C15), 20.1 (C18). HMRS (DART) m/z [C₄₈H₃₂N₂]⁺ calcd. 637.2643, found 637.2627.

1,4-bis(carbazol-9-yl)phenyl)ethynyl)-2,5-dimethylbenzene (2-d₈)

The same procedure for **1** was used to prepare **2-d₈** using the following amounts: N-(4-iodophenyl)carbazole (**2-d₄**) (0.500 g, 1.33 mmol), 1,4-diethynyl-2,5-dimethylbenzene (**3**) (0.104 g, 0.677 mmol), PdCl₂(PPh₃)₂ (0.094 g, 0.133 mmol), CuI (0.012 g, 0.066 mmol), dry THF (6 mL). The resulting product was yellow solid (0.258 g, 60 %, M.P by DCS 278-285 °C). ¹H NMR (300 MHz, CDCl₃) δ : 8.15 (d, 4H, ³J = 7.7 Hz) 7.47-7.39 (m, 10H), 7.33-7.29 (m, 4H), 2.55 (s, 3H). ¹³C NMR (75 MHz, CDCl₃) δ : 140.6 (C9a), 137.5 (C10), 137.4 (C17), 132.8 (C19), 126.1 (C2), 123.6 (C4a), 123.0 (C16) 122.1 (C13), 120.4 (C4), 120.3 (C3), 109.7 (C1), 93.9 (C14), 89.3 (C15), 20.7 (C18). HMRS (DART) m/z [C₄₈H₂₅²H₈N₂]⁺ calcd. 645.31459, found 645.31324.

N-(4-Iodophenyl)carbazole (3)

In a two-neck round-bottom flask a mixture of carbazole (0.500 g, 2.99 mmol), 1,4-diiodobenzene (1.97 g, 5.98 mmol), CuI (0.028 g, 0.14 mmol), 18-crown-6 (0.013 g, 0.04 mmol), K₂CO₃ (0.826 g, 5.97 mmol) and *N, N'*-Dimethylpropylene urea (6 mL) was heated to 140 °C and stirred for 1 h under nitrogen atmosphere. Then, at room temperature the mixture was quenched with water, and the resulting precipitate was filtered. The resulting product was dissolved in dichloromethane and then washed with 30 mL of saturated solution of NH₄Cl, and the organic phase was extracted with dichloromethane (3x20 mL). The combined organic layers were dried over Na₂SO₄, and the

solvent was removed by evaporation. The resulting solid was purified by column chromatography using hexanes as eluent to afford compound **3** as a white solid (0.930 g, 85%, M. P. 139-141 °C). Spectral data were consistent with literature reports.⁹

N-(4-Iodophenyl)carbazole (**3-d₄**)

The same procedure for **3** was used to prepare **3-d₄** using the following amounts: carbazole (0.500g, 2.99 mmol), 1,4-diiodobenzene-*d*₄ (0.458 g, 1.49 mmol), CuI (0.028 g, 0.14 mmol), 18-crown-6 (0.013 g, 0.04 mmol), K₂CO₃ (0.826 g, 5.97 mmol) and *N,N'*-dimethylpropylene urea (3 mL) was heated to 140 °C and stirred for 1 h under nitrogen atmosphere according with the previous methodology. The resulting product was beige (0.880g, 80 %, M. P. 139–141 °C), and the spectral data were consistent with literature reports.⁹

1,4-bis(ethynyl)-2,5-dimethylbenzene (4)

In a one-neck round bottom flask a mixture of 1,4-Bis(trimethylsilyl)ethynyl-2,5-dimethylbenzene (**5**) (0.500 g, 1.67 mmol), K₂CO₃ (0.462 g, 3.34 mmol) and methanol (10 mL) was stirred for 4 h at room temperature, then the mixture was treated with a saturated solution of NaHCO₃ and the organic phase was extracted with dichloromethane (3x30 mL). The combined organic layers were dried over Na₂SO₄ then the solvent was removed by evaporation. The resulting residue was purified by column chromatography using hexanes as eluent to afford compound **4** as brown solid (0.232 g, 90 %, M.P. 98 - 100 °C). IR ν_{max} : 3265, 2952, 2920, 2853, 2096, 1930, 1486, 14343, 1265, 1035, 893, 648, 623. ¹H NMR (300 MHz, CDCl₃) δ : 7.30 (s, 1H), 3.32 (s, 1H), 2.28 (s, 3H). ¹³C NMR (75 MHz, CDCl₃) δ : 140.6, 139.3, 100.6, 26.9. HMRS (DART) *m/z* [C₁₂H₁₀]⁺ calcd. 155.0860, found 155.0862.

1,4-Bis(trimethylsilyl)ethynyl-2,5-dimethylbenzene (5)

To a one-neck round-bottom flask was added 1,4-diiodo-2,5-dimethylbenzene (**6**) (0.500 g, 1.39 mmol), PdCl₂(PPh₃)₂ (0.098 g, 0.139 mmol), CuI (0.013 g, 0.069 mmol), ethynyltrimethylsilane (0.342 g, 3.49 mmol), dry THF (6 mL) and triethylamine (1 mL) under nitrogen atmosphere. Then the reaction mixture was stirred for 3 h at room temperature, after this time the mixture was washed

9. A. Aguilar-Granda, S. Pérez-Estrada, A. E. Roa, J. Rodríguez-Hernández, S. Hernández-Ortega, M. Rodríguez, B. Rodríguez-Molina, *Cryst. Growth Des.*, 2016, **16**, 3435-3442.

with 30 mL of saturated solution of NH_4Cl and extracted with dichloromethane (3x30 mL). The combined organic layers were dried over Na_2SO_4 and the solvent was removed under vacuum. The crude product was purified by column chromatography using hexanes as solvent. The compound **5** was obtained as yellow solid (0.417 g, 95 %, M. P. 87-89 °C). IR ν_{max} : 2955, 2923, 2853, 2152, 1488, 1452, 1248, 1206, 837, 757, 624. ^1H NMR (300 MHz, CDCl_3) δ : 7.25 (s, 2H), 2.34 (s, 6H), 0.25 (s, 18H). ^{13}C NMR (75 MHz, CDCl_3) δ : 137.7, 133.0, 123.1, 104.0, 100.0, 20.0, 0.18. HMRS (DART) m/z [$\text{C}_{18}\text{H}_{26}\text{Si}_2$] $^+$ calcd. 299.1651, found 299.1651.

1,4-diiodo-2,5-dimethylbenzene (6)

In a two-neck round-bottom flask under nitrogen atmosphere, NaIO_4 (1.2 g, 5.61 mmol), and crystals of I_2 (3.2 g, 14.9 mmol) were suspended in a mixture of glacial AcOH (15 mL) and Ac_2O (10 mL), and stirred 15 min at 0 °C using an ice/salt bath. Then, 2.5 mL of H_2SO_4 was added dropwise during 1 h, taking care that the temperature does not exceed 10 °C. After this time, 1 mL of *p*-xylene (0.865 g, 8.14 mmol) was added dropwise, and the reaction mixture was warmed to room temperature and stirred for 4 h. After that time, the mixture was poured into a 50 mL of an aqueous saturated solution of Na_2SO_3 . The precipitate was filtrated and recrystallized with EtOH to give a white solid (2.6 g, 90 %, M.P. 78-80 °C). IR ν_{max} : 2970, 2909, 1743, 1463, 1430, 1035, 875, 430. ^1H NMR (300 MHz, CDCl_3) δ : 7.6 (s, 2H), 2.3 (s, 6H). ^{13}C NMR (75 MHz, CDCl_3) δ : 140.6, 139.2, 100.6, 26.9. HMRS (DART) m/z [$\text{C}_8\text{H}_8\text{I}_2$] $^+$ calcd. 357.8715, found 357.8730.

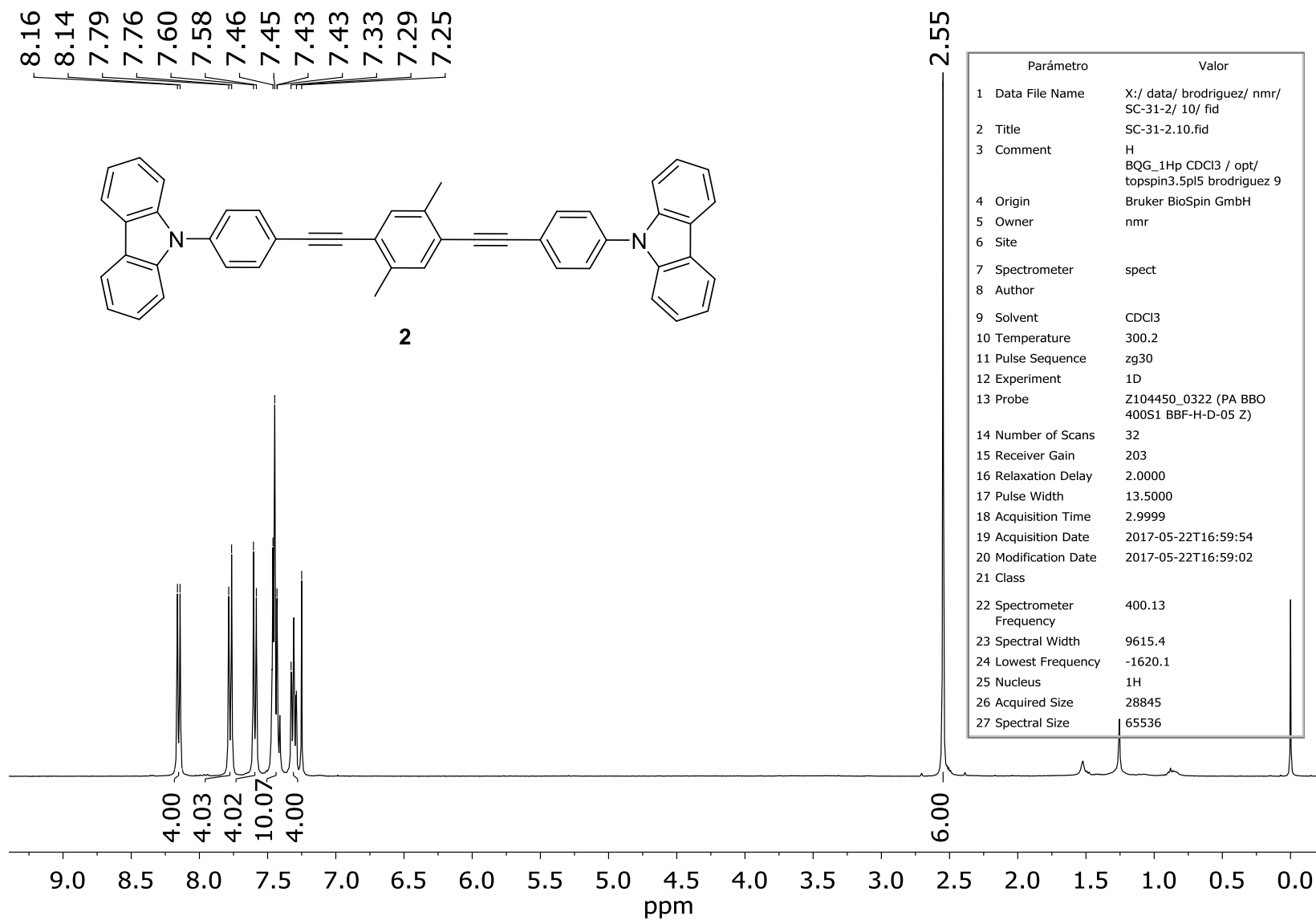


Figure S26. ¹H NMR (400 MHz) spectrum of compound **2** in CDCl₃

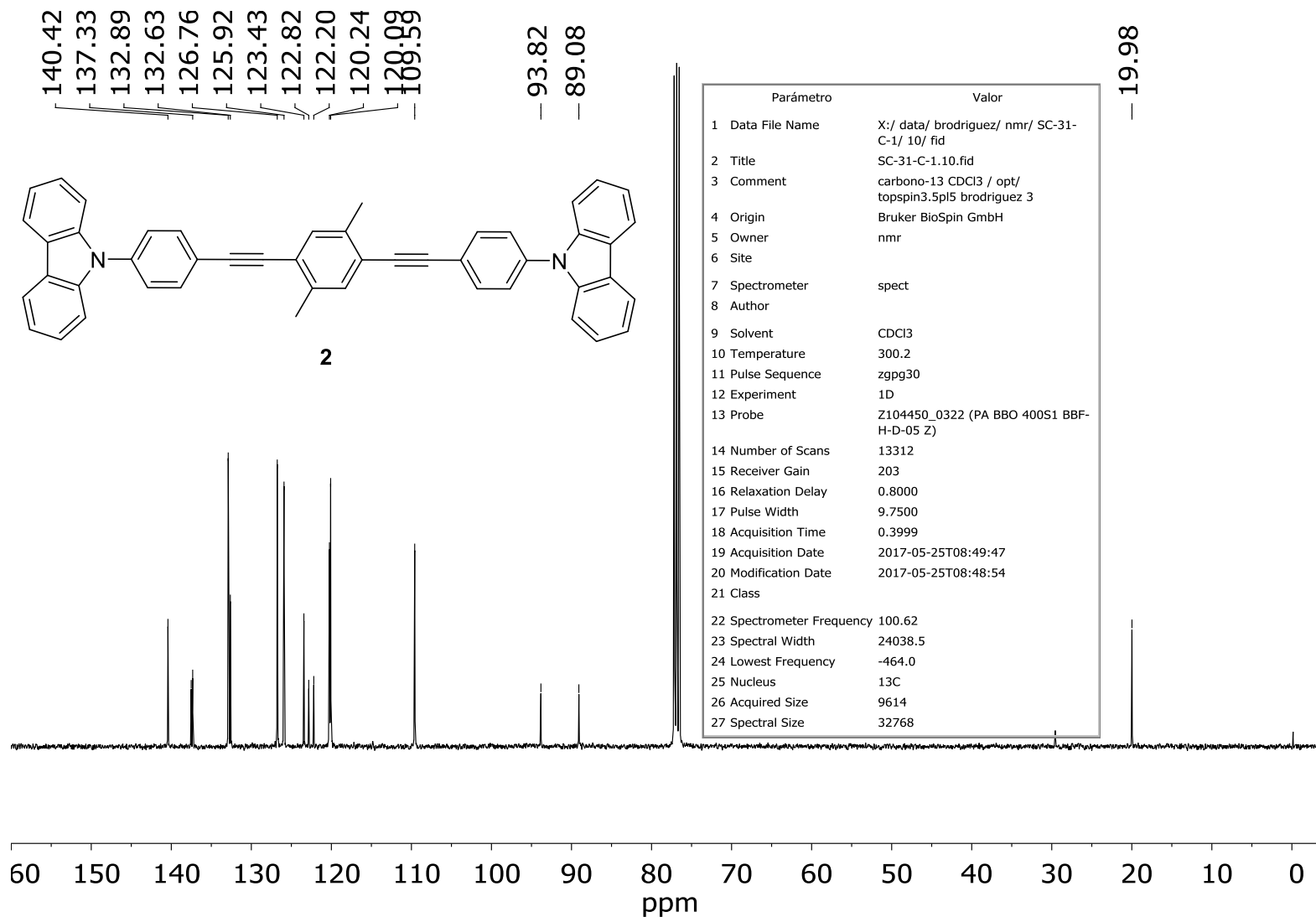


Figure S27. ^{13}C NMR (100 MHz) spectrum of compound **2** in CDCl_3

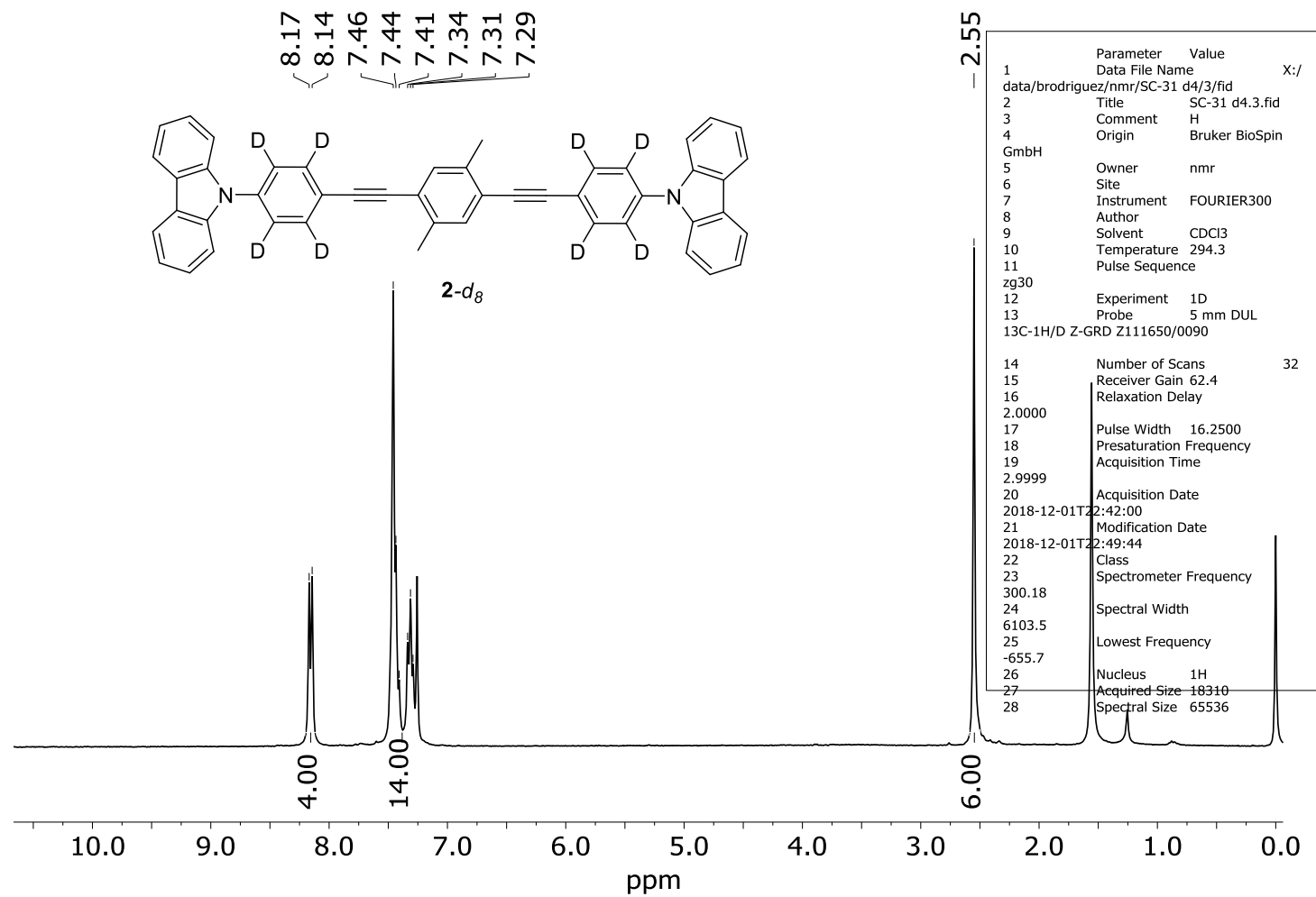


Figure S28. ¹H NMR (300 MHz) spectrum of compound **2-d₈** in CDCl₃

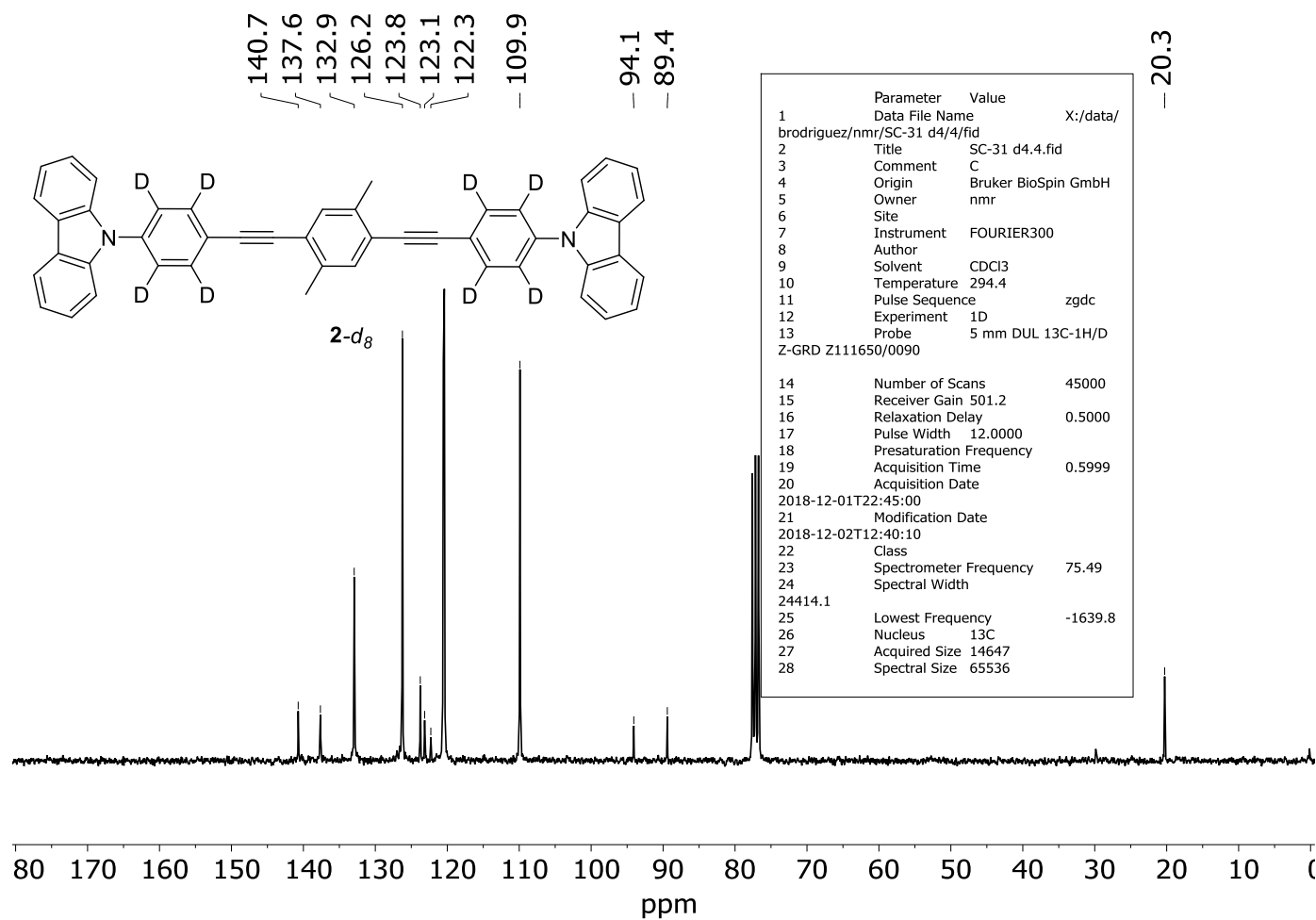


Figure S29. ¹³C NMR (75 MHz) spectrum of compound **2-d₈** in CDCl₃

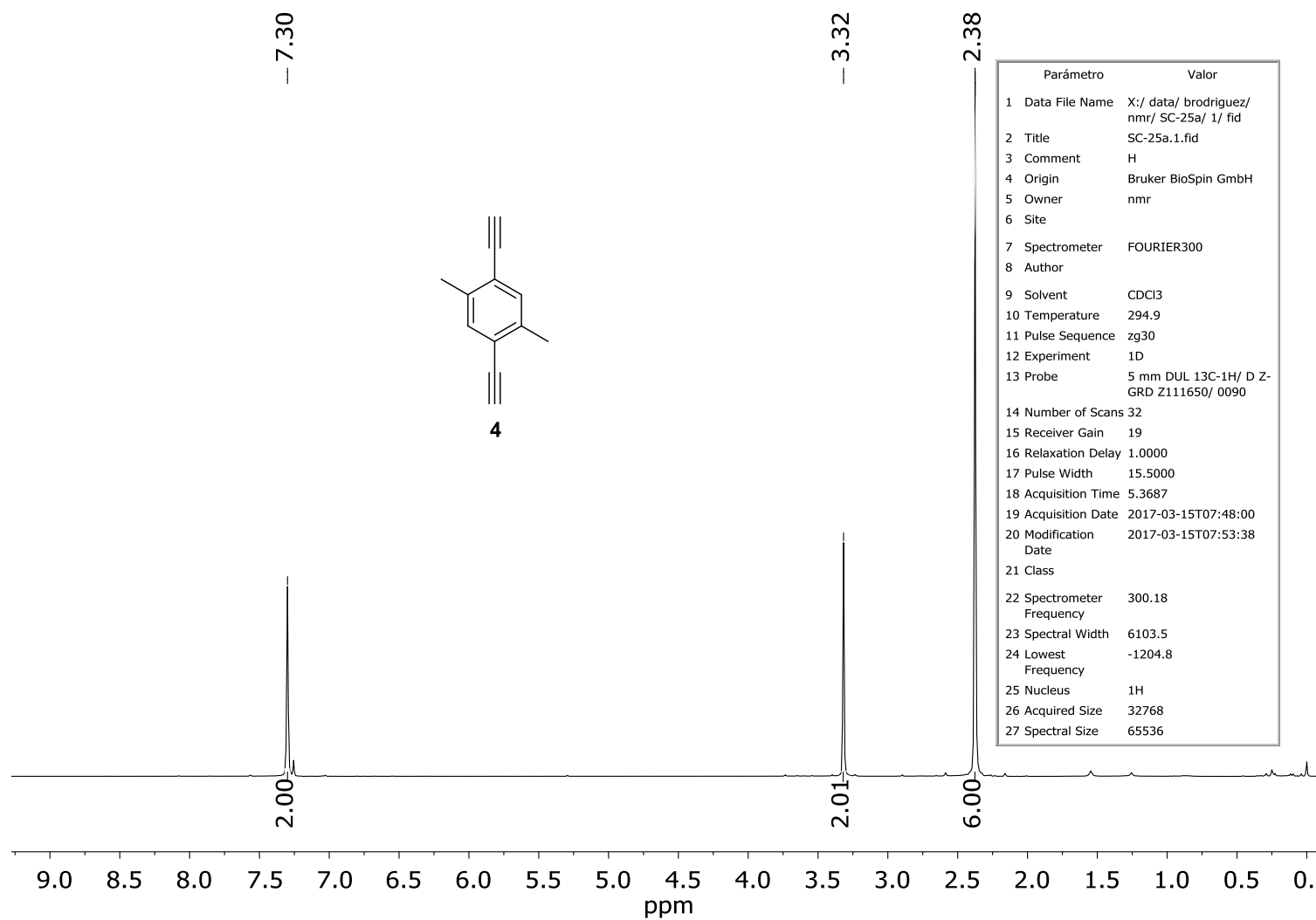


Figure S30. ¹H NMR (300 MHz) spectrum of compound **4** in CDCl₃

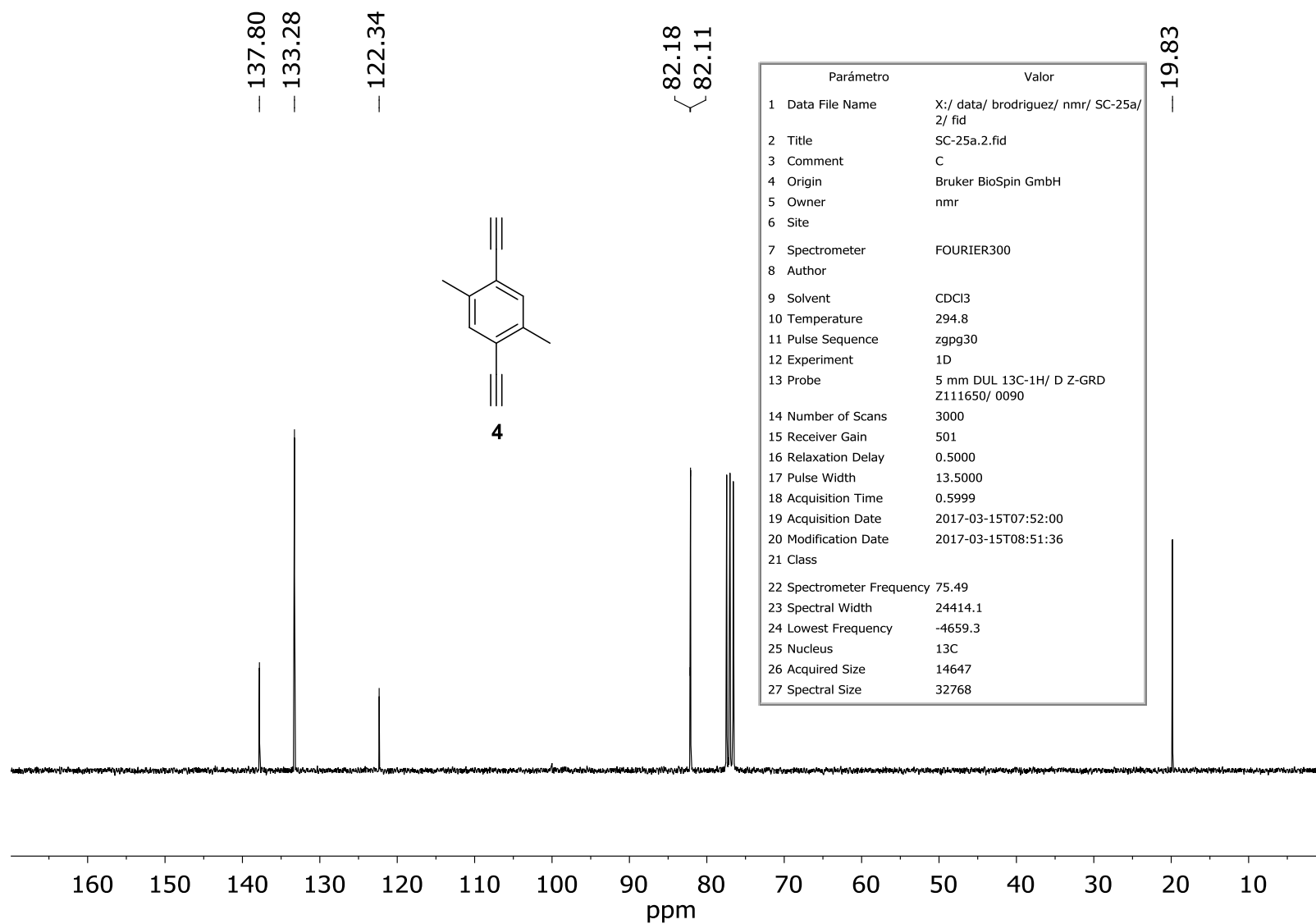


Figure S31. ^{13}C NMR (75 MHz) spectrum of compound **4** in CDCl_3

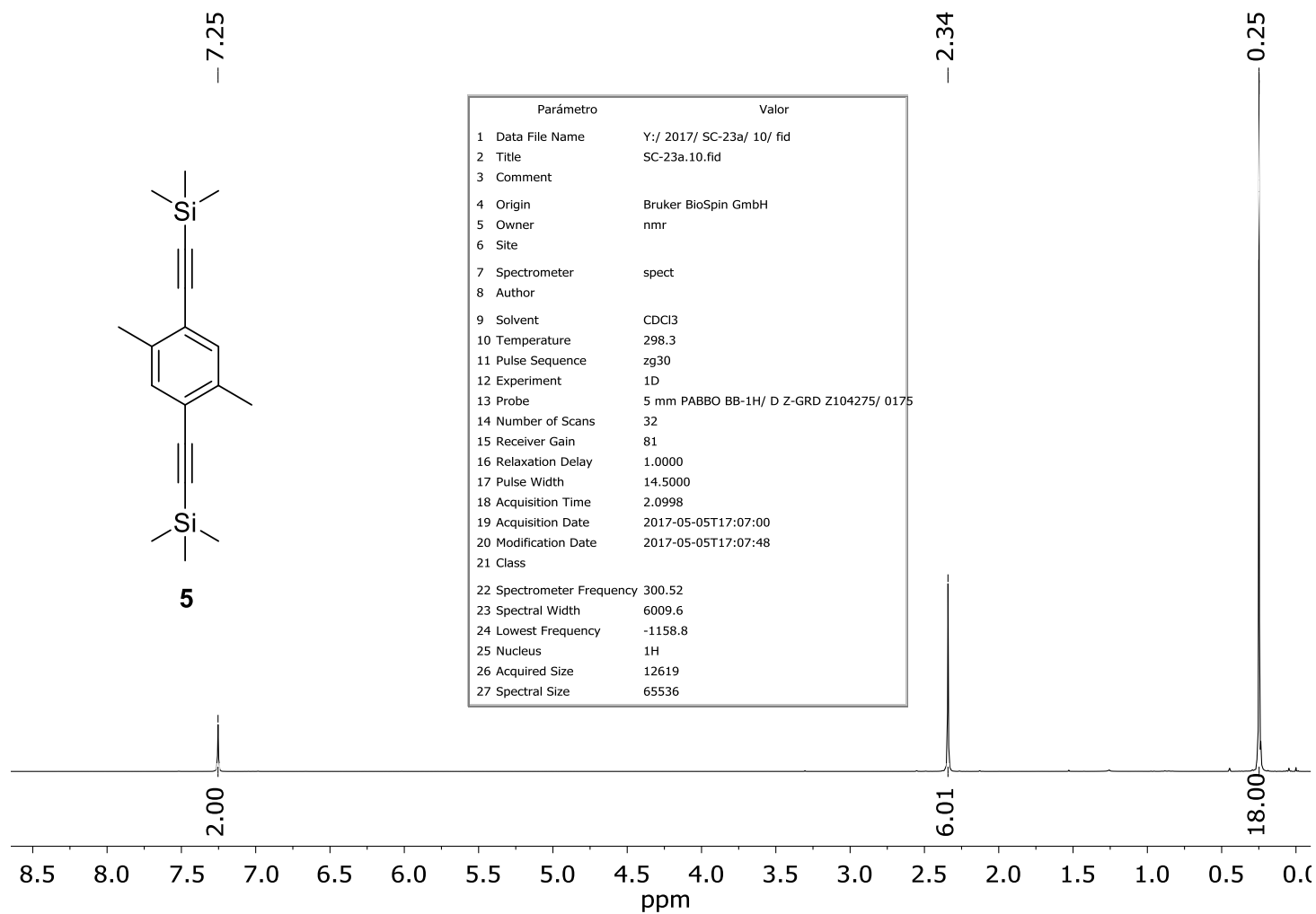


Figure S32. ^1H NMR (300 MHz) spectrum of compound **5** in CDCl_3

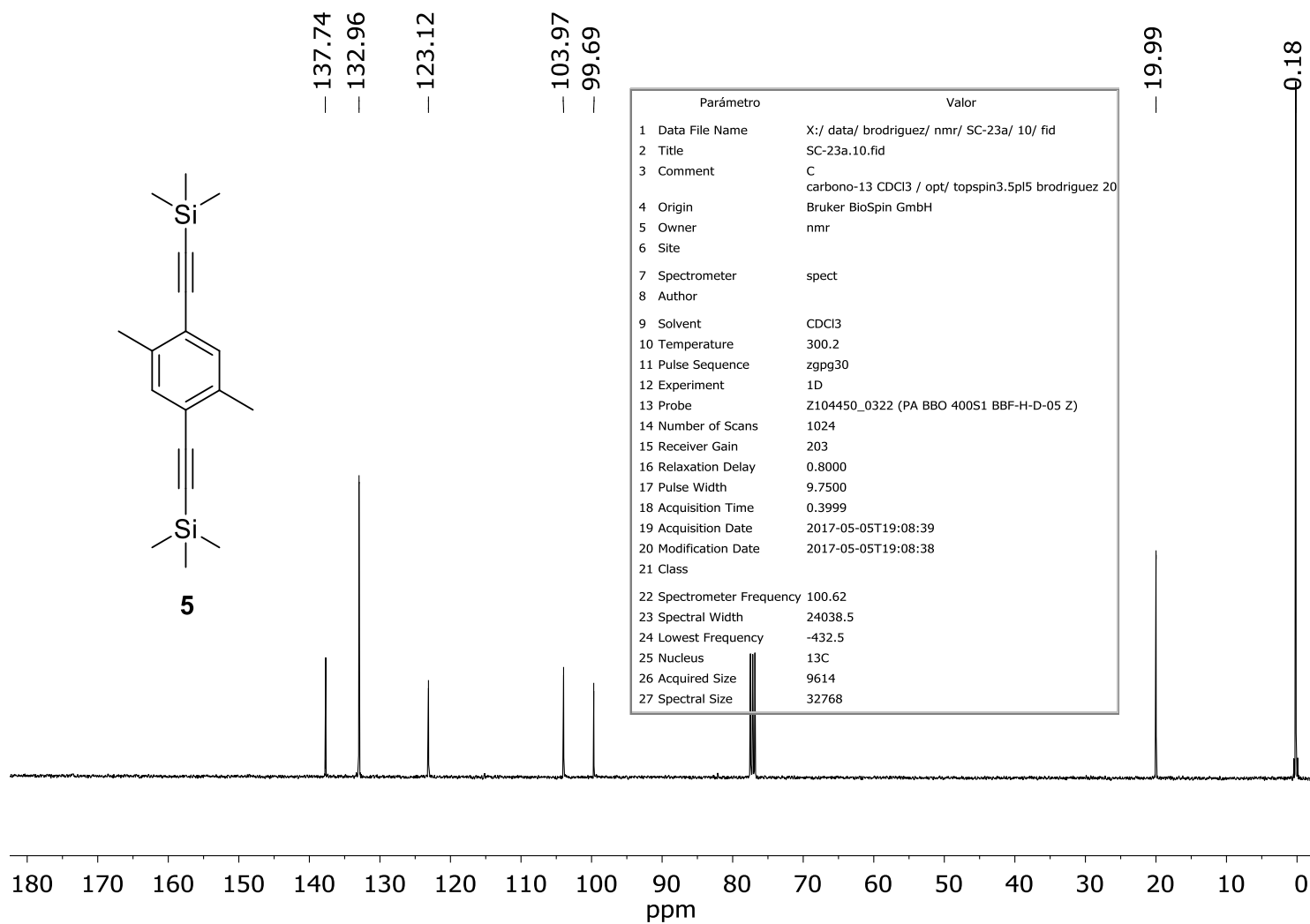


Figure S33. ¹³C NMR (100 MHz) spectrum of compound **5** in CDCl₃

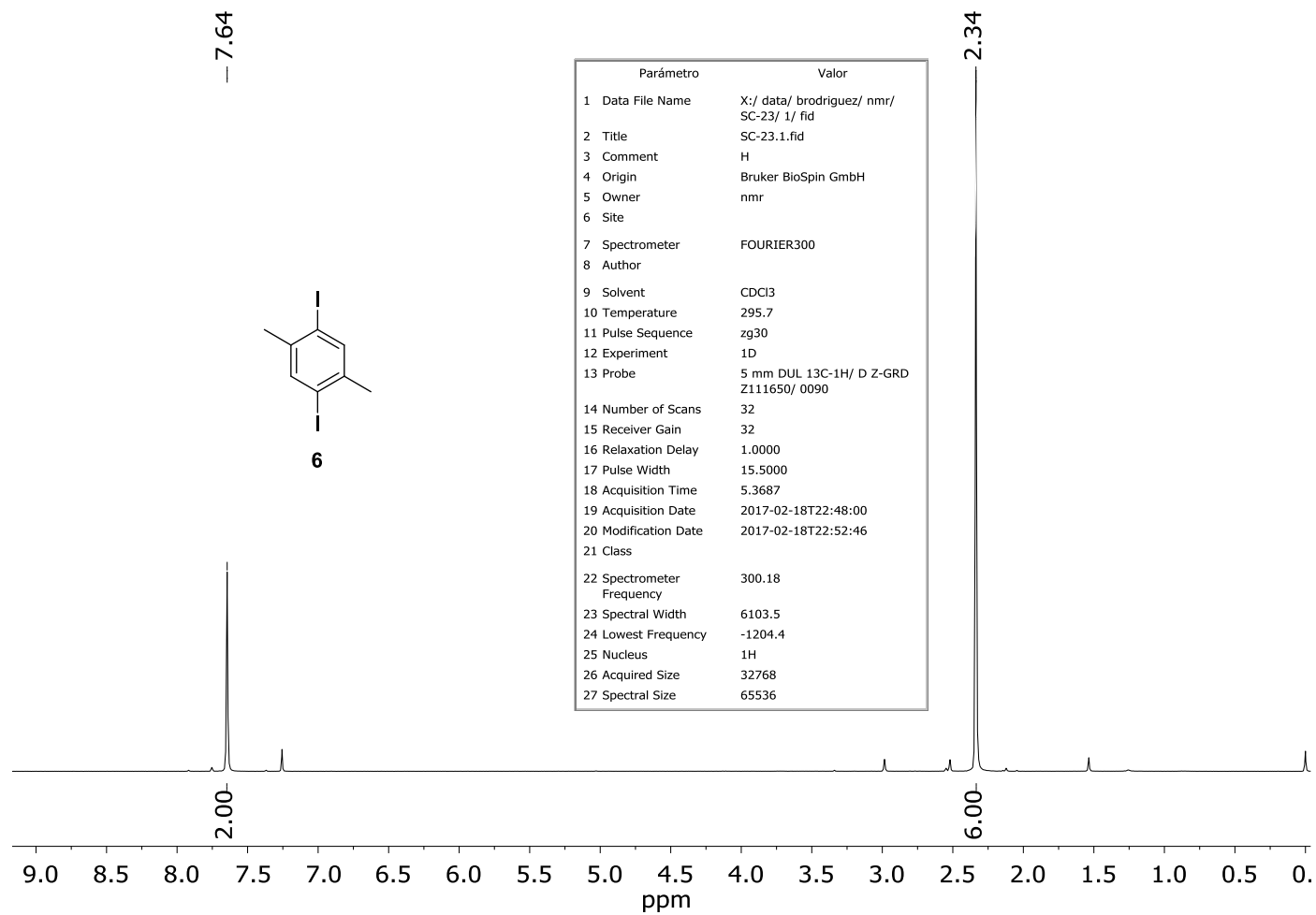


Figure S34. ^1H NMR (300 MHz) spectrum of compound **6** in CDCl_3

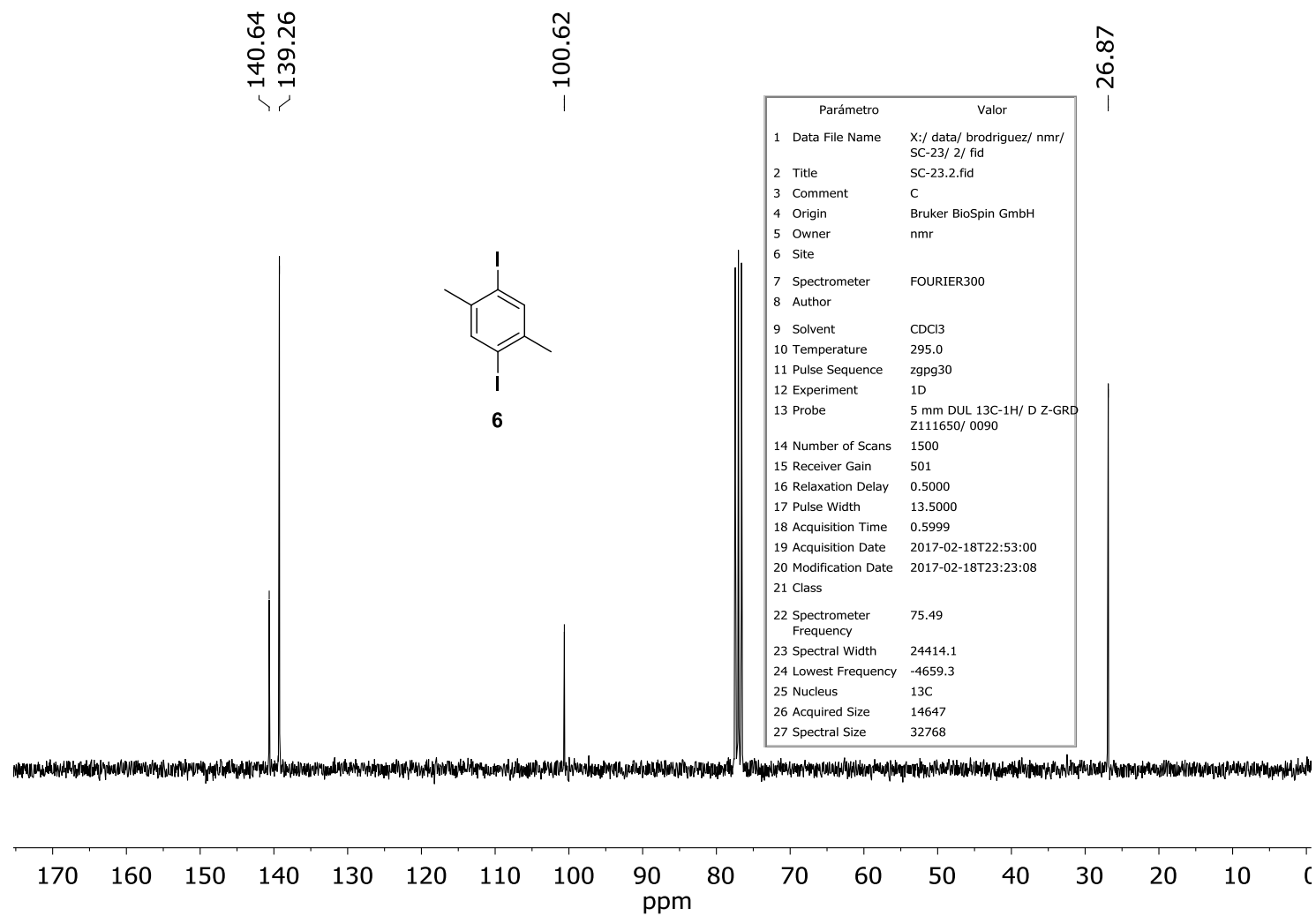


Figure S35. ^{13}C NMR (75 MHz) spectrum of compound **6** in CDCl_3